

# Charge and spin gaps of the ionic Hubbard model with density-dependent hopping

O. A. Moreno Segura

*Centro Atómico Bariloche and Instituto Balseiro, 8400 Bariloche, Argentina*

K. Hallberg

*Instituto de Nanociencia y Nanotecnología CNEA-CONICET,  
Centro Atómico Bariloche and Instituto Balseiro, 8400 Bariloche, Argentina*

A. A. Aligia

*Instituto de Nanociencia y Nanotecnología CNEA-CONICET, GAIDI,  
Centro Atómico Bariloche and Instituto Balseiro, 8400 Bariloche, Argentina*

We calculate the charge gap  $\Delta E_C$  and the spin gap  $\Delta E_S$  of the ionic Hubbard chain including electron-hole symmetric density-dependent hopping. The vanishing of  $\Delta E_C$  ( $\Delta E_S$ ) signals a quantum critical point (QCP) in the charge (spin) sector. Between both critical points, the system is a fully gapped spontaneously dimerized insulator (SDI). We focus our study in this region. Including alternation in the hopping, it is possible to perform an adiabatic Thouless pump of one charge per cycle, but with a velocity limited by the size of the gaps.

## I. INTRODUCTION

The ionic Hubbard model (IHM) consists of the usual Hubbard model with on-site Coulomb repulsion  $U$  supplemented by an alternating one-particle potential  $\Delta$ . It has been used to study the neutral-to-ionic transition in organic charge-transfer salts<sup>1,2</sup> and the ferroelectric transition<sup>3</sup>. More recent studies have established that the chain has three different thermodynamic phases, and different gaps, correlation functions and other properties have been studied<sup>4–12</sup>. Here we assume half filling. The unit cell consists of two sites with on-site energies  $\pm\Delta$ . Chains with larger unit cells have also been studied<sup>13,14</sup>.

The model has three phases, the band insulating (BI), the Mott insulating (MI) and a narrow spontaneously dimerized insulating (SDI) phase in between. An intuitive understanding of the first two phases is provided by the zero-hopping limit, in which the occupancies of the different sites are like 2020... (BI phase) for  $\Delta > U/2$  and 1111... (MI phase) for  $\Delta < U/2$ . For finite hopping the SDI phase appears in between, as first shown by bosonization<sup>4</sup>, and described in more detail later using an approximate mapping to an SU(3) Heisenberg model<sup>8,9</sup>.

The phase diagram of the model has been constructed in Ref. 5 using the method of crossings of excited energy levels (MCEL) based on conformal field theory<sup>15–19</sup>. For this model (including also density-dependent hopping) the method also coincides with that of jumps of charge and spin Berry phases used in Ref. 20. The basis of the MCEL is that in one dimension, the dominant correlations at large distances correspond to the smallest excitation energies. Thus, the crossings of excited levels in appropriate symmetry sectors therefore correspond to phase transitions. Lanczos using total wave vector, inversion symmetry<sup>21</sup> and time-reversal symmetry has been used in order to separate the different symmetry sectors, limiting the maximum size to 16 sites. The results were obtained extrapolating to the thermo-

dynamic limit<sup>5</sup>. Open-shell boundary conditions (OSBC) were used, which correspond to periodic BC for a number of sites  $L$  multiple of 4, and antiperiodic BC for even  $L$  not multiple of 4.

For fixed  $U$ , small  $\Delta$ , and half-filling as assumed here, the system is in the MI phase with zero spin gap. Increasing  $\Delta$ , at the point  $\Delta = \Delta_s$ , a spin gap  $\Delta E_S$  opens signaling the transition to the SDI phase. the transition is of the Kosterlitz-Thouless type<sup>4</sup>. Although the spin gap is exponentially small near the transition, the MCEL allows to identify it unambiguously and accurately from the crossing of the even singlet with lowest energy and the odd triplet of lowest energy (both states have higher energy than the ground state)- At  $\Delta = \Delta_s$ , also the spin Berry phase  $\gamma_s^{5,20}$  jumps from  $\pi$  to  $0 \bmod(2\pi)$ . Further increasing  $\Delta$ , rather soon, at the point  $\Delta = \Delta_c$  a charge transition from the SDI to the BI phase takes place in which the charge reorders. At this point, there is a crossing of the two singlets of lowest energy with opposite parity under inversion. In the BI phase the ground state is the singlet even under inversion, while it is the odd singlet in the other two phases. All these states have wave vector 0 for  $\Delta \neq 0$ . In turn, this crossing leads to a jump in the charge Berry phase  $\gamma_c$  from  $\pi$  to  $0 \bmod(2\pi)$ . As explained above, for  $\Delta = \Delta_c$  and using OSBC, the charge gap  $\Delta E_C$  defined as the absolute value of difference in energy between the ground state and the first excited state at half filling (in other works called exciton gap<sup>6</sup> or internal gap<sup>31</sup>) vanishes at the charge transition.

Changes in  $\gamma_c$  are proportional to changes in the polarization. Actually, calculations of the charge Berry phase form the basis of the modern theory of polarization<sup>22–30</sup>. A jump in  $\pi$  in  $\gamma_c$  is consistent with a displacement of an electronic charge per unit cell in half a unit cell (to the next site) on average. This is the change of polarization that corresponds to the change in site occupancies from 1111.. to 2020... The IHM in a ring has inversion symmetry with center at any site<sup>21</sup>, and as a consequence

$\gamma_c$  and  $\gamma_s$  can only be 0 or  $\pi \bmod(2\pi)$ . In other words, they are  $Z_2$  topological numbers protected by inversion symmetry<sup>30</sup>.

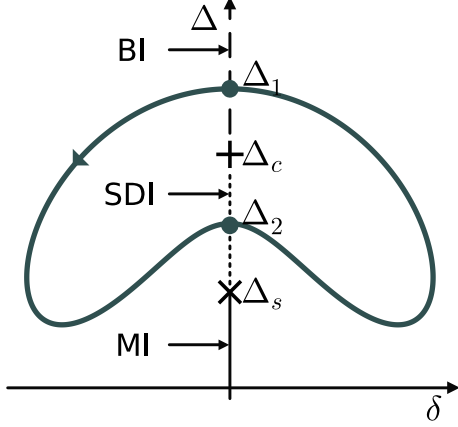


FIG. 1. Schematic representation of the pump trajectory. Dashed, dotted, and solid lines indicate the BI, SDI and MI phases of the IHM (at  $\delta = 0$ ), respectively.

If a modulation of the hopping  $\delta$  is introduced, the inversion symmetry is lost, and  $\gamma_c$  can change continuously. This permits to transfer one charge to the next unit cell in a Thouless pump cycle in the  $(\Delta, \delta)$  plane (see Fig. 1). This can be understood as follows. Starting at a point  $(\Delta_1, 0)$  with  $\Delta_1 > \Delta_c$ ,  $\gamma_c = 0$ . Then introducing a finite  $\delta$ , with the appropriate sign,  $\gamma_c$  increases continuously with increasing  $|\delta|$ . Decreasing  $\Delta$  to a value  $\Delta_2 < \Delta_c$  and returning  $\delta$  to zero, the point  $(\Delta_2, 0)$  is reached where  $\gamma_c = \pi$ . Continuing the cycle with the opposite sign of  $\delta$ ,  $\gamma_c$  continues to increase and reaches the value  $\gamma_c = 2\pi$  at the end of the cycle at  $(\Delta_1, 0)$ . This corresponds to the displacement of one unit charge by one unit cell according to the modern theory of polarization. The values of the Berry phases in the cycle and time-dependent calculations of the charge transferred have been presented in Ref. 31. Moreover, this pumping procedure has been realized experimentally recently<sup>32</sup>, allowing to study the effects of interactions in the field of quantized topological charge pumping in driven systems, which is of great interest in the last years<sup>33,34</sup>.

A problem with the pumping cycle mentioned above is that it usually crosses the MI segment between the points  $(\Delta_s, 0)$  and  $(-\Delta_s, 0)$  at which the spin gap vanishes. Since unavoidably this segment is traversed at a finite speed, spin excitations are created, leading to the loss of adiabatic quantized pumping<sup>31,32</sup> (we note that introducing  $\delta$  in the MI phase, a spin gap  $\Delta E_S$  opens proportional to  $|\delta|^{2/3}$  for small  $\delta$ <sup>31</sup>). To avoid this problem, one might choose the crossing point  $\Delta_2$  inside the SDI phase, that is  $\Delta_s < \Delta_2 < \Delta_c$  (as it is shown in Fig. 1), and then the system is fully gapped in the whole trajectory. However, at  $\Delta = \Delta_2$  both gaps  $\Delta E_C$  and  $\Delta E_S$  are small, and their magnitude is not known. Previous

calculations of  $\Delta E_S$  were affected by strong finite-size effects in the SDI region and were limited to very large values of  $U$ <sup>6</sup>. On the other hand, it has been recently shown that the SDI phase is enlarged at small values of  $U$  if density dependent hopping is introduced<sup>35</sup>. A density-dependent hopping can be experimentally engineered by near-resonant Floquet modulation<sup>36–40</sup>.

In this work, we calculate both gaps,  $\Delta E_C$  and  $\Delta E_S$  inside and near the SDI phase, and explore the optimum value of  $\Delta_2$  for which the smallest gap is maximum. We use density-matrix renormalization group (DMRG)<sup>54–58</sup>, as described in Section III. We find that to calculate  $\Delta E_S$  open BC are more convenient, while to calculate  $\Delta E_C$ , a ring with OSBC leads to the optimum results, improving previous estimates and allowing to calculate the charge gap within the SDI phase with unprecedented accuracy.

The paper is organized as follows. In Section II we briefly explain the model. In Section III, we describe the methods used to calculate the gaps. The results are presented in Section IV. Section V contains a summary and discussion.

## II. MODEL

The model we study here is the IHM with density-dependent hopping (DDH). It is the version without alternation of the hopping ( $\delta = 0$ ) of the interacting Rice-Mele model<sup>41</sup> including DDH. Because of its relevance for quantized charge pumping, we describe the full Hamiltonian including also  $\delta$  below

$$\begin{aligned}
 H = & \sum_{j\sigma} [-1 + \delta (-1)^j] (c_{j\sigma}^\dagger c_{j+1\sigma} + \text{H.c.}) \\
 & \times [t_{AA}(1 - n_{j\bar{\sigma}})(1 - n_{j+1\bar{\sigma}}) + t_{BB}n_{j\bar{\sigma}}n_{j+1\bar{\sigma}} \\
 & + t_{AB}(n_{j\bar{\sigma}} + n_{j+1\bar{\sigma}} - 2n_{j\bar{\sigma}}n_{j+1\bar{\sigma}})] \\
 & + \Delta \sum_{j\sigma} (-1)^j n_{j\sigma} + U \sum_j n_{j\uparrow} n_{j\downarrow}.
 \end{aligned} \tag{1}$$

The first term is the DDH, which is alternating for  $\delta \neq 0$ . The amplitudes  $t_{AA}$ ,  $t_{AB}$  and  $t_{BB}$  correspond to hopping of a particle with a given spin, when the total occupancy of both sites for particles with the opposite spin is 0, 1 and 2 respectively. In the following we assume the electron-hole symmetric case  $t_{BB} = t_{AA}$ , which is the one implemented experimentally with cold atoms<sup>36–40</sup>.  $\Delta$  is the alternating on-site energy and  $U$  is the on-site Coulomb repulsion.

The model with  $\Delta = \delta = 0$  has been derived and studied in two dimensions as an effective model for cuprate superconductors<sup>42–45</sup>. In one dimension also superconductivity is favored for some parameters<sup>46–50</sup>. Our interest in DDH here is that for  $t_{AB}$  larger than the other two, the fully gapped SDI phase is favored<sup>18,20,35,51,52</sup>. This is important for fully adiabatic quantized charge pumping of one charge. So far, charge pumping has been studied

in the interacting Rice-Mele model in absence of DDH ( $t_{AA} = t_{AB} = t_{BB}$ )<sup>31,32,34,53</sup>.

### III. METHODS

To perform the energy level calculations, we have used the DMRG method with a code that relies on the ITensors library for Julia<sup>59</sup>. Conveniently setting  $S_z$  sectors, we have calculated ground and excited states with a fixed bond dimension of 900. The truncation error is, in the worst case, on the order of  $10^{-6}$  for periodic BC (PBC), and  $10^{-10}$  for open BC (OBC).

In general, it is convenient to use OBC rather than PBC, because the entanglement is lower in the former case, leading to more accurate results in less amount of time. In turn, this fact permits to reach larger systems. This is particularly important for the spin gap  $\Delta E_S$ , because even in regions of parameters for which  $\Delta E_S = 0$  in the thermodynamic limit, it is finite for finite systems, scaling as  $1/L$  for increasing system size  $L$ <sup>15</sup>. We have calculated the spin gap by extrapolating the results for different system sizes using a quadratic function in  $1/L$ . The calculations were done for systems between  $L = 40$  and  $L = 100$ , except in the case of  $U = 10$ , where we have used sizes up to  $L = 64$ .

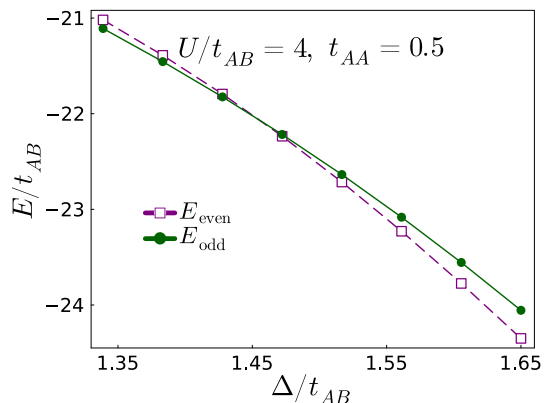


FIG. 2. (Color online) Ground state and first excited state as a function of  $\Delta$  for 32 sites and PBC.

For the charge gap  $\Delta E_C$ , which is the difference of energies between the first excited state and the ground state in the singlet sector, the situation is different. For OBC we find similar difficulties as those found before<sup>6</sup> for calculating the gap in the SDI phase and particularly near the transition to the BI phase, where it should vanish in the thermodynamic limit. The reason is the following. As it is clear using the MCEL method mentioned in Section I, the ground state and the first excited state have opposite parity under inversion, being the even state the one of lowest energy in the BI phase, and both states cross at the BI-SDI transition. For a chain with OBC

and an integer number of unit cells, the inversion symmetry is lost, the crossing becomes an anticrossing, and extrapolation to the thermodynamic limit becomes problematic. Therefore, we change the method using a ring with OSBC as described below.

The Lanczos method used in the MCEL has divided the Hilbert space in different symmetry sectors, but the method is limited to 16 sites at half filling<sup>5,18,35</sup>. Our method allows us to use larger system sizes, but we do not have access to the different symmetry sectors. In any case, just plotting the energy of the ground state and first excited state as a function of  $\Delta$  in a ring, both energy levels and the crossing can be clearly identified. This is illustrated in Fig. 2 for a typical case.  $t_{AB} = 1$  is chosen as the unit of energy. We find that extrapolating the energies of  $L$  multiple of 4 for a ring with PBC (which coincide with OSBC for the chosen  $L$ ) between  $L = 12$  and  $L = 32$  using a quadratic function in  $1/L$ , an accurate and reliable result for  $\Delta E_C$  in the thermodynamic limit is obtained. An example of the extrapolation is presented in Fig. 3

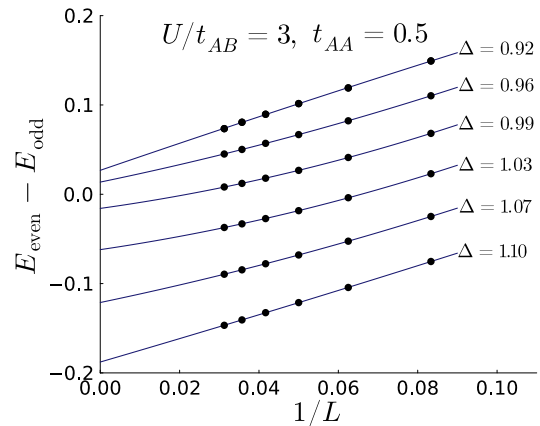


FIG. 3. Difference of energy between the even and odd states of lowest energy as a function of the inverse of the systems size  $L$  for all  $L$  multiple of 4 in the range  $12 \leq L \leq 32$  with PBC for several values of  $\Delta$ . The transition is calculated to be at  $\Delta_c = 0.978$ .

Noting that the slopes of the gap are different at both sides of the transition, we find that the difference between odd and even states can be well fitted by the following function with three parameters

$$E_{\text{odd}} - E_{\text{even}} = (\Delta - \Delta_c) \left[ A + \tanh \left( \frac{\Delta - \Delta_c}{B} \right) \right]. \quad (2)$$

Examples will be shown in the next Section.

Comparing with previous results using the MCEL in smaller systems<sup>35</sup>, we have also found that using OSBC, the crossing between the first excited state in the sector with total spin projection  $S_z = 0$  (corresponding to the even singlet<sup>35</sup>) and the lowest-energy state in the sector

with  $S_z = 1$  (an odd triplet<sup>35</sup>) corresponds to the crossing at  $\Delta = \Delta_s$  that signals the opening of the spin gap  $\Delta E_S$ , and the SDI-MI transition, as explained in Section I.

Therefore, our methods might be also used to improve the accuracy of phase diagrams calculated with the MCEL, extending the results to larger systems.

We have found empirically, that sufficiently far from  $\Delta_s$  and in the SDI phase, or in the BI phase near the SDI-BI transition at  $\Delta = \Delta_c$ , the dependence on  $\Delta$  of the spin gap is well described by the expression

$$\Delta E_S = A_s \exp[B_s(\Delta - C_s)]. \quad (3)$$

#### IV. RESULTS

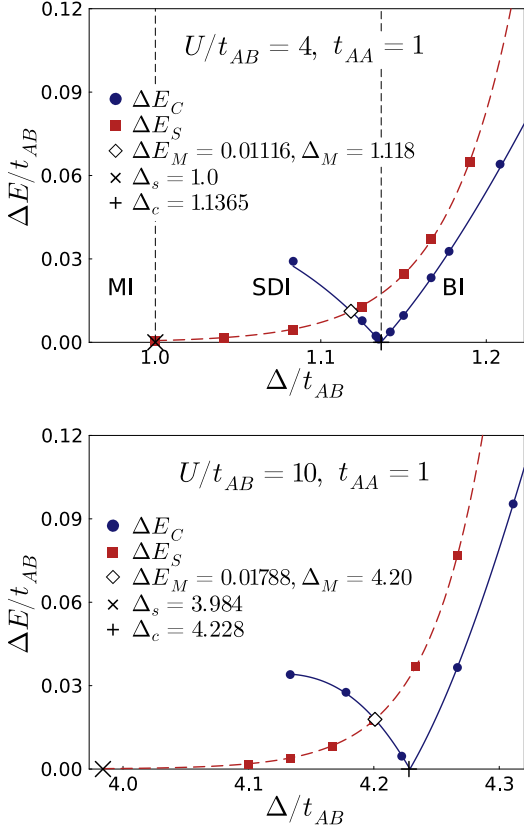


FIG. 4. (Color online) Charge gap (blue circles) and spin gap (red squares) as a function of  $\Delta$  for two values of  $U$  and  $t_{AA} = t_{BB} = t_{AB} = 1$ . Blue solid [red dashed] line is a fit using Eq. (2) [Eq. (3)]. Vertical lines in the top figure separate the different phases of the IHM.

In Fig. 4, we show the gaps for the model without DDH and two values of  $U$ . The maximum difference between any excited state and the ground state in the SDI phase is denoted by  $\Delta E_M$ . This value is obtained at the crossing between both studied gaps. The value of  $\Delta$

at this crossing is denoted as  $\Delta_M$ . We take  $t_{AB} = 1$  as the unit of energy.

From the figure, one can see that the spread of the SDI phase  $\Delta_c - \Delta_s$  and also  $\Delta E_M$  are larger for larger values of  $U$  than for moderate ones. The former fact is in agreement with calculations of the phase diagram using up to 16 sites<sup>5</sup>, although  $\Delta_c - \Delta_s$  is a little bit smaller in our case. Our values should be more accurate since we have calculated  $\Delta_c$  and  $\Delta_s$  using up to 32 and 28 sites, respectively.

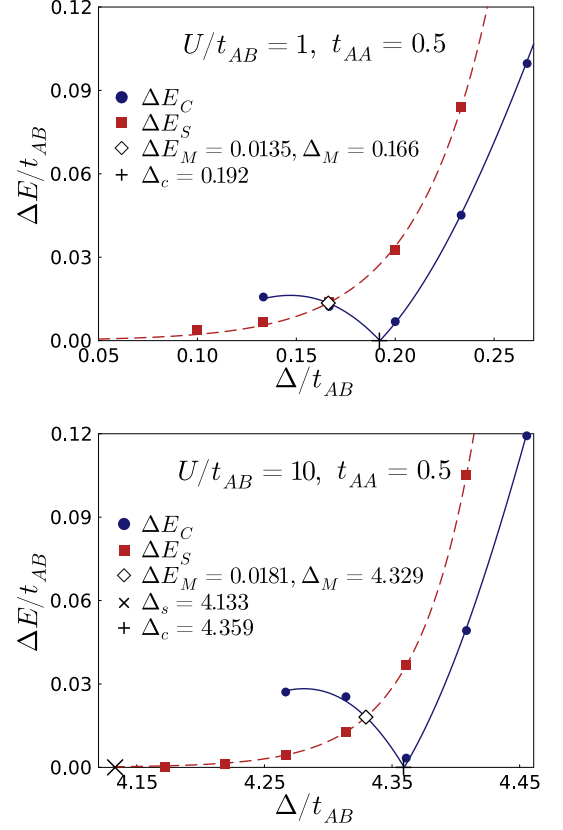


FIG. 5. (Color online) Same as Fig. 4 for  $t_{AA} = t_{BB} = 0.5$  and  $t_{AB} = 1$ .

In Fig. 5 we analyze the effect of DDH, decreasing  $t_{AA} = t_{BB}$  to half the value of  $t_{AB} = 1$ , for two extreme values of  $U$ , leaving the intermediate values of  $U$  for Fig. 6. For  $U = 10$ , the maximum value of the gap  $\Delta E_M$  *increases* slightly. This effect is rather surprising, because one naively expects that reducing the average value of the hopping, both  $\Delta E_M$  and the amplitude of the SDI phase should decrease. Therefore, the effect of introducing DDH overcomes the effect of reducing the average hopping regarding  $\Delta E_M$ . Instead, the amplitude of the SDI phase  $\Delta_c - \Delta_s$  decreases slightly.

As discussed earlier<sup>35</sup>, for small values of  $U$ , the amplitude of the SDI phase increases strongly, since it continues to exist even for  $\Delta = 0$ . However, the magnitude of the maximum gap  $\Delta E_M$  is reduced by 25% when  $U$  is

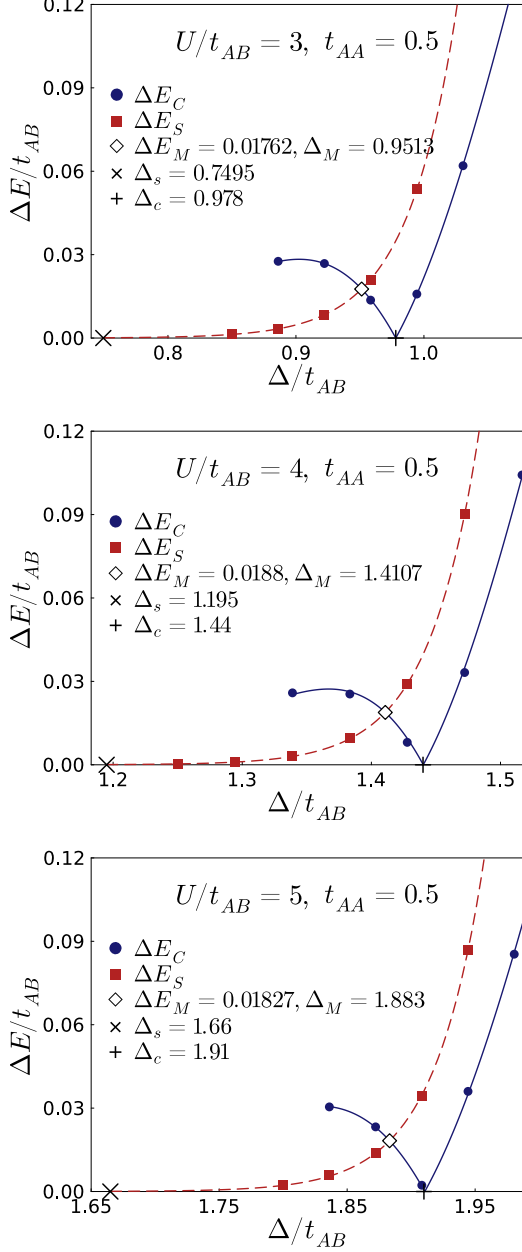


FIG. 6. (Color online) Same as Fig. 5 for intermediate values of  $U$ .

reduced from 10 to 1 in units of  $t_{AB}$ .

In order to look for the largest possible value of  $\Delta E_M$  in presence of DDH, we have calculated the gaps for intermediate values of  $U$ . The result is shown in Fig. 6.

While qualitatively, the results for  $U = 3, 4$  and  $5$  are similar, the maximum gap  $\Delta E_M = 0.0188$  is obtained for  $U = 4$ .

## V. SUMMARY AND DISCUSSION

We have calculated the charge and spin gaps of the spontaneously dimerized insulating (SDI) phase of the ionic Hubbard model, including electron-hole symmetric density-dependent hopping. We have developed a new method using DMRG to calculate the charge gap, which presents advantages with respect to previously used ones, leading to substantially more accurate values. In addition, phase diagrams constructed by the method of crossing of energy levels might be calculated more accurately than using only Lanczos methods, if they are combined with DMRG (the former can be used to identify the symmetry sectors).

The results might be useful to present experiments with cold atoms in which quantized Thouless pumping of one charge is observed, when a pump cycle in the two-dimensional space  $(\Delta, \delta)$  enclosing the point  $(\Delta_c, 0)$  is performed in a realization of the interacting Rice-Mele model [Eq. (1)], where  $\Delta_c$  is the value of  $\Delta$  at the transition between the SDI and the band insulating (BI) phase. A fully adiabatic pump is possible if the Mott insulating (MI) phase is avoided. This phase lies at the segment between the points  $(\Delta_s, 0)$  and  $(-\Delta_s, 0)$ , where  $\pm\Delta_s$  are the points of the MI-SDI phase transitions. For this purpose, the SDI phase should be traversed.

Fixing  $t_{AB} = 1$  we find that the maximum gap inside the SDI phase is about 0.019. This is a rather small value, which by simple estimates seems to require a velocity about 10 times smaller than that used in available experiments<sup>32</sup> to guarantee adiabatic pumping in crossing the point  $(\Delta_M, 0)$ . However introducing  $\delta$  the gap increases quickly (as  $|\delta|^{2/3}$  in the MI phase). A time-dependent calculation, possibly decreasing the velocity near  $(\Delta_M, 0)$  would be useful to check this procedure.

The effect of density-dependent hopping, reducing  $t_{AA} = t_{BB}$  and keeping  $t_{AB} = 1$  is moderate in increasing the gap, although it is important if the average hopping is kept at the same value. Its main effect is that for small  $U$ , the extension of the fully gapped SDI phase is strongly increased.

## ACKNOWLEDGMENTS

AAA (KH) acknowledges financial support provided by PICT 2017-2726 and PICT 2018-01546 (PICT 2018-01546) of the ANPCyT, Argentina. KH acknowledges support from ICTP through the Associates Programs.

<sup>1</sup> Nagaosa and J. Takimoto, Theory of Neutral-Ionic Transition in Organic Crystals. I. Monte Carlo Simulation of

Modified Hubbard Model, J. Phys. Soc. Jpn. **55**, 2735 (1986).

- <sup>2</sup> Hubbard and J.B. Torrance, Model of the Neutral-Ionic Phase Transformation, *Phys. Rev. Lett.* **47**, 1750 (1981).
- <sup>3</sup> T. Egami, S. Ishihara, and M. Tachiki, Lattice effect of strong electron correlation: Implication for ferroelectricity and superconductivity, *Science* **261**, 1307 (1993).
- <sup>4</sup> M. Fabrizio, A.O. Gogolin, and A.A. Nersisyan, From Band Insulator to Mott Insulator in One Dimension, *Phys. Rev. Lett.* **83**, 2014 (1999).
- <sup>5</sup> M. E. Torio, A. A. Aligia, and H. A. Ceccatto, Phase diagram of the Hubbard chain with two atoms per cell, *Phys. Rev. B* **64**, 121105(R) (2001).
- <sup>6</sup> S. R. Manmana, V. Meden, R. M. Noack, and K. Schönhammer, Quantum critical behavior of the one-dimensional ionic Hubbard model, *Phys. Rev. B* **70**, 155115 (2004).
- <sup>7</sup> A. A. Aligia, Charge dynamics in the Mott insulating phase of the ionic Hubbard model, *Phys. Rev. B* **69**, 041101(R) (2004).
- <sup>8</sup> C. D. Batista and A. A. Aligia, Exact Bond Ordered Ground State for the Transition between the Band and the Mott Insulator, *Phys. Rev. Lett.* **92**, 246405 (2004).
- <sup>9</sup> A. A. Aligia and C. D. Batista, Dimerized phase of ionic Hubbard models, *Phys. Rev. B* **71**, 125110 (2005).
- <sup>10</sup> L. Tincani, R. M. Noack, and D. Baeriswyl, Critical properties of the band-insulator-to-Mott-insulator transition in the strong-coupling limit of the ionic Hubbard model, *Phys. Rev. B* **79**, 165109 (2009).
- <sup>11</sup> A. Hosseinzadeh and S. A. Jafari, Quantum Integrability of 1D Ionic Hubbard Model, *Ann. der. Phys.* **532**, 1900601 (2020).
- <sup>12</sup> A. Hosseinzadeh and S. A. Jafari, Generalization of Lieb–Wu wave function inspired by one-dimensional ionic Hubbard model, *Annals of Physics* **414**, 168075 (2020).
- <sup>13</sup> M. E. Torio, A. A. Aligia, G. I. Japaridze, and B. Normand, Quantum phase diagram of the generalized ionic Hubbard model for  $AB_n$  chains, *Phys. Rev. B* **73**, 115109 (2006).
- <sup>14</sup> L. Stenzel, A. L. C. Hayward, C. Hubig, U. Schollwöck, and F. Heidrich-Meisner, Quantum phases and topological properties of interacting fermions in one-dimensional superlattices, *Phys. Rev. A* **99**, 053614 (2019).
- <sup>15</sup> K. Nomura and K. Okamoto, Critical properties of  $S=1/2$  antiferromagnetic XXZ chain with next-nearest-neighbour interactions, *J. Phys. A* **27**, 5773 (1994).
- <sup>16</sup> M. Nakamura, K. Nomura, and A. Kitazawa, Renormalization Group Analysis of the Spin-Gap Phase in the One-Dimensional  $t-J$  Model, *Phys. Rev. Lett.* **79**, 3214 (1997).
- <sup>17</sup> M. Nakamura, Mechanism of CDW-SDW Transition in One Dimension, *J. Phys. Soc. Jpn.* **68**, 3123 (1999).
- <sup>18</sup> M. Nakamura, Tricritical behavior in the extended Hubbard chains, *Phys. Rev. B* **61**, 16377 (2000).
- <sup>19</sup> R. D. Somma and A. A. Aligia, Phase diagram of the XXZ chain with next-nearest-neighbor interactions, *Phys. Rev. B* **64**, 024410 (2001).
- <sup>20</sup> A. A. Aligia, K. Hallberg, C.D. Batista and G. Ortiz, Phase diagrams from topological transitions: The Hubbard chain with correlated hopping, *Phys. Rev. B* **61**, 7883 (2000).
- <sup>21</sup> The inversion symmetry in a ring of  $L$  sites with center at site  $i$  is defined as the operation which interchanges the sites  $i-j$  and  $i+j \bmod(L)$  for all  $j$ .
- <sup>22</sup> R. Resta, Macroscopic polarization in crystalline dielectrics: the geometric phase approach. *Rev. Mod. Phys.* **66**, 899 (1994).
- <sup>23</sup> D. Xiao, M.-C. Chang, and Q. Niu, Berry phase effects on electronic properties, *Rev. Mod. Phys.* **82**, 1959 (2010).
- <sup>24</sup> D. Vanderbilt, *Berry Phases in Electronic Structure Theory: Electric Polarization, Orbital Magnetization and Topological Insulators*, (Cambridge University Press, 2018).
- <sup>25</sup> B. Bradlyn, and M. Iraola, Lecture notes on Berry phases and topology, *SciPost Phys. Lect. Notes* 51 (2022).
- <sup>26</sup> G. Ortiz and R. M. Martin, Macroscopic polarization as a geometric quantum phase: Many-body formulation, *Phys. Rev. B* **49**, 14202 (1994).
- <sup>27</sup> R. Resta and S. Sorella, Many-Body Effects on Polarization and Dynamical Charges in a Partly Covalent Polar Insulator, *Phys. Rev. Lett.* **74**, 4738 (1995).
- <sup>28</sup> G. Ortiz, P. Ordejón, R. M. Martin, and G. Chiappe, Quantum phase transitions involving a change in polarization, *Phys. Rev. B* **54**, 13515 (1996).
- <sup>29</sup> X.-Y. Song, Y.-C. He, A. Vishwanath, and C. Wang, Electric polarization as a nonquantized topological response and boundary Luttinger theorem, *Phys. Rev. Research* **3**, 023011 (2021).
- <sup>30</sup> A. A. Aligia, Topological invariants based on generalized position operators and application to the interacting Rice-Mele model, *Phys. Rev. B* **107**, 075153 (2023).
- <sup>31</sup> E. Bertok, F. Heidrich-Meisner, and A. A. Aligia, Splitting of topological charge pumping in an interacting two-component fermionic Rice-Mele Hubbard model, *Phys. Rev. B* **106**, 045141 (2022).
- <sup>32</sup> K. Viebahn, A-S Walter, E. Bertok, Z. Zhu, M. Gächter, A. A. Aligia, F. Heidrich-Meisner, and T. Esslinger, Interaction-induced charge pumping in a topological many-body system, *arXiv:2308.03756*
- <sup>33</sup> R. Citro and M. Aidelsburger, Thouless pumping and topology, *Nat. Rev. Phys.* **5**, 87 (2023).
- <sup>34</sup> A.-S. Walter, Z. Zhu, M. Gächter, J. Minguzzi, S. Roschinski, K. Sandholzer, K. Viebahn, and T. Esslinger, Breakdown of quantisation in a Hubbard-Thouless pump, *Nat. Phys.* (2023), 10.1038/s41567-023-02145-w.
- <sup>35</sup> P. Roura-Bas and A. A. Aligia, P. Roura-Bas and A. A. Aligia, Phase diagram of the ionic Hubbard model with density-dependent hopping, *Phys. Rev. B* in press (<https://arxiv.org/abs/2304.04563>)
- <sup>36</sup> R. Ma, M. E. Tai, P. M. Preiss, W. S. Bakr, J. Simon, and M. Greiner, Photon-assisted tunneling in a biased strongly correlated Bose gas, *Phys. Rev. Lett.* **107**, 095301 (2011).
- <sup>37</sup> F. Meinert, M. J. Mark, K. Lauber, A. J. Daley, and H.-C. Nägerl, Floquet engineering of correlated tunneling in the Bose-Hubbard model with ultracold atoms, *Phys. Rev. Lett.* **116**, 205301 (2016).
- <sup>38</sup> F. Görg, M. Messer, K. Sandholzer, G. Jotzu, R. Desbuquois, and T. Esslinger, Enhancement and sign change of magnetic correlations in a driven quantum many-body system *Nature* **553**, 481 (2018).
- <sup>39</sup> M. Messer, K. Sandholzer, F. Görg, J. Minguzzi, R. Desbuquois, and T. Esslinger, Floquet Dynamics in Driven Fermi-Hubbard Systems *Phys. Rev. Lett.* **121**, 233603 (2018).
- <sup>40</sup> F. Görg, K. Sandholzer, J. Minguzzi, R. Desbuquois, M. Messer, and T. Esslinger, Realization of density-dependent Peierls phases to engineer quantized gauge fields coupled to ultracold matter, *Nature Physics* **15**, 1161 (2019).
- <sup>41</sup> M. J. Rice and E. J. Mele, Elementary Excitations of a Linearly Conjugated Diatomic Polymer, *Phys. Rev. Lett.* **49**, 1455 (1982).
- <sup>42</sup> H.B. Schüttler and A.J. Fedro, Copper-oxygen charge excitations and the effective-single-band theory of cuprate

- superconductors, *Phys. Rev. B* **45**, 7588 (1992).
- <sup>43</sup> M. E. Simon and A. A. Aligia, Brinkman-Rice transition in layered perovskites, *Phys. Rev. B* **48**, 7471 (1993).
- <sup>44</sup> J.E. Hirsch and F. Marsiglio, Hole superconductivity: Review and some new results, *Physica C: Supercond. Appl.* **62-164**, 591 (1989).
- <sup>45</sup> L. Arrachea and A. A. Aligia, Pairing correlations in a generalized Hubbard model for the cuprates, *Phys. Rev. B* **61**, 9686 (2000).
- <sup>46</sup> A. A. Aligia, A. Anfossi, L. Arrachea, C. Degli Esposti Boschi, A. O. Dobry, C. Gazza, A. Montorsi, F. Ortolani, and M. E. Torio, Incommensurability and Unconventional Superconductor to Insulator Transition in the Hubbard Model with Bond-Charge Interaction, *Phys. Rev. Lett.* **99**, 206401 (2007).
- <sup>47</sup> A. O. Dobry and A. A. Aligia, Quantum phase diagram of the half filled Hubbard model with bond-charge interaction *Nucl. Phys. B* **843**, 767 (2011).
- <sup>48</sup> A. Montorsi, U. Bhattacharya, Daniel González-Cuadra, M. Lewenstein, G. Palumbo, and L. Barbiero, Interacting second-order topological insulators in one-dimensional fermions with correlated hopping, *Phys. Rev. B* **106**, L241115 (2022).
- <sup>49</sup> W. Chen, J. Zhang, and H. Ding, Ground-state instabilities in a Hubbard-type chain with particular correlated hopping at non-half-filling, *Results in Physics*, 106472 (2023).
- <sup>50</sup> S. Jiang, D. J. Scalapino, and S. R. White, A single-band model with enhanced pairing from DMRG-based downfold-  
ing of the three-band Hubbard model, arXiv:2303.00756
- <sup>51</sup> G. I. Japaridze and A. P. Kampf, Weak-coupling phase diagram of the extended Hubbard model with correlated-hopping interaction, *Phys. Rev. B* **59**, 12822 (1999).
- <sup>52</sup> A. A. Aligia and L. Arrachea, Triplet superconductivity in quasi-one-dimensional systems *Phys. Rev. B* **60**, 15332 (1999).
- <sup>53</sup> M. Nakagawa, T. Yoshida, R. Peters, and N. Kawakami, Breakdown of topological Thouless pumping in the strongly interacting regime, *Phys. Rev. B* **98**, 115147 (2018).
- <sup>54</sup> S. R. White, Density matrix formulation for quantum renormalization groups, *Phys. Rev. Lett.* **69**, 2863 (1992).
- <sup>55</sup> K. A. Hallberg, New trends in density matrix renormalization. *Adv. Phys.* **55**, 477 (2006)
- <sup>56</sup> U. Schollwöck, The density-matrix renormalization group, *Rev. Mod. Phys.* **77**, 259 (2005)
- <sup>57</sup> U. Schollwöck, The density-matrix renormalization group in the age of matrix product states, *Ann. Phys.* **326**, 96 (2011)
- <sup>58</sup> M. C. Bañuls, Tensor Network Algorithms: A Route Map, *Annual Review of Cond. Matt. Phys.* **14**, 173 (2023)
- <sup>59</sup> M. Fishman, S. White and E. Stoudenmire, The ITensor software library for tensor network calculations. *SciPost Phys. Codebases*, **4** (2022).